THE JOURNAL OF BIOLOGICAL CHEMISTRY VOL. 287, NO. 50, pp. 42019–42030, December 7, 2012

Serine 363 Is Required for Nociceptin/Orphanin FQ Opioid Receptor (NOPR) Desensitization, Internalization, and Arrestin Signaling*

Received for publication, July 31, 2012, and in revised form, October 17, 2012 Published, JBC Papers in Press, October 19, 2012, DOI 10.1074/jbc.M112.405696

Nancy R. Zhang[‡1], William Planer[‡1], Edward R. Siuda[‡§], Hu-Chen Zhao[‡], Lucy Stickler[‡], Steven D. Chang[‡], Madison A. Baird[‡], Yu-Qing Cao[‡§¶], and Michael R. Bruchas[‡§¶‖2]

From the [‡]Department of Anesthesiology, Basic Research Division, and [‖]Department of Anatomy and Neurobiology, [¶]Washington University Pain Center, [§]Division of Biology and Biomedical Sciences, Program in Neuroscience, Washington University School of Medicine, St. Louis, Missouri 63110

Background: Nociceptin/orphanin FQ opioid receptors (NOPR) are the least understood member of the opioid G protein-coupled receptor family.
Results: NOPR serine 363 is required for receptor internalization, desensitization, and c-Jun N-terminal (JNK) phosphorylation.
Conclusion: NOPR is regulated via GRK3 and Arrestin3 to control G-protein-dependent and -independent signaling.
Significance: Understanding NOPR signaling and regulation could provide novel clues to the development of functionally selective opioid receptor ligands.

We determined the role of carboxyl-terminal regulation of NOPR (nociceptin, orphanin FQ receptor) signaling and function. We mutated C-terminal serine and threonine residues and examined their role in NOPR trafficking, homologous desensitization, and arrestin-dependent MAPK signaling. The NOPR agonist, nociceptin, caused robust NOPR-YFP receptor internalization, peaking at 30 min. Mutation of serine 337, 346, and 351, had no effect on NOPR internalization. However, mutation of C-terminal threonine 362, serine 363, and threonine 365 blocked nociceptin-induced internalization of NOPR. Furthermore, point mutation of only Ser-363 was sufficient to block NOPR internalization. Homologous desensitization of NOPR-mediated calcium channel blockade and inhibition of cAMP were also shown to require Ser-363. Additionally, NOPR internalization was absent when GRK3, and Arrestin3 were knocked down using siRNA, but not when GRK2 and Arrestin2 were knocked down. We also found that nociceptin-induced NOPR-mediated JNK but not ERK signaling requires Ser-363, GRK3, and Arrestin3. Dominant-positive Arrestin3 but not Arrestin2 was sufficient to rescue NOPR-S363A internalization and JNK signaling. These findings suggest that NOPR function may be regulated by GRK3 phosphorylation of Ser-363 and Arrestin3 and further demonstrates the complex nature of G-protein-dependent and -independent signaling in opioid receptors.

Nociceptin/orphanin FQ receptor (NOPR)[3] (also called Opioid receptor like-1, ORL1) is the most recently identified member of the opioid receptor family and least understood of the four receptor subtypes. NOPR receptors are widely expressed throughout the brain and spinal cord and are activated by the endogenous peptide nociceptin (1–3). Through coupling to the G-protein $G\alpha_{i/o}$, NOPR inhibits adenylate cyclase, and decreases N-type $Ca_V2.2$ calcium conductances (4–6). The mechanisms of NOPR signal transduction are still under active investigation. NOPR receptor regulation has been only briefly studied and it is known that activation of NOPR with nociceptin produces rapid and robust receptor internalization over time (7). For the other three opioid receptor types it has been established that carboxyl-terminal serine residues are phosphorylated by G protein-coupled receptor kinases (GRK), followed by recruitment of endocytic machinery via the binding of arrestin. This process effectively results in receptor-G-protein inactivation and subsequent receptor internalization (2). However, little is known regarding the mechanisms of NOPR phosphorylation, internalization, and desensitization.

For many GPCR members, it is widely known that sustained agonist activation can lead to receptor phosphorylation and internalization (8). For the NOPR receptor the key amino acid residues, kinetics, and arrestin/GRK proteins involved remain unresolved. In addition, over the last decade, evidence suggests that arrestin-bound GPCR is not inactive but instead recruits a whole host of noncanonical signaling modules (9–12). For example, for the κ-opioid receptor and μ-opioid receptors, β-arrestins (also called Arrestin2 and -3) are involved in p38 and ERK mitogen-activated protein kinase (MAPK) activation (10, 13, 14). Activation and recruitment of the third arm of the MAPK family, c-Jun N-terminal kinase (JNK) pathway has also been shown to require arrestin in some GPCR systems (15–17). JNK signaling has been demonstrated to play a role in the stress

* This work was supported, in whole or in part, by National Institutes of Health Grants R00DA034929 (to M. R. B.) and T32DA007261 (to S. D. C.) and the Howard Hughes Medical Institute SURF Fellowship Program (to N. Z. and L. S.).
[1] Both authors contributed equally to this work.
[2] To whom correspondence should be addressed: Dept. of Anesthesiology and Anatomy-Neurobiology, Washington University School of Medicine, 660 South Euclid Ave., St. Louis, MO 63110. Tel.: 314-747-5754; E-mail: bruchasm@wustl.edu.
[3] The abbreviations used are: NOPR, nociceptin/orphanin FQ opioid peptide receptor; NOP, nociceptin/orphanin FQ opioid peptide; DP-Arr, dominant-positive Arrestin; pJNK, phosphorylated c-Jun N-terminal kinase; GRK, G-protein coupled receptor kinase; ANOVA, analysis of variance; qRT, quantitative RT; GPCR, G protein-coupled receptor.

response, apoptotic cell signaling, neurodegeneration, and ischemia (18).

To assess how NOPR receptors are dynamically regulated, desensitized, and whether they activate arrestin-dependent MAPK pathways, we first determined key carboxyl-terminal amino acid residues required for NOPR internalization and desensitization of G-protein signaling. Here we show that the key residue for NOPR regulation is serine 363. We next expressed NOPR-YFP and NOPR-S363A-YFP into HEK293 cells and determined the kinetics and properties of receptor internalization, desensitization of $Ca_V2.2$ regulation, and cAMP inhibition. Furthermore, we assessed the role of serine 363 in GRK/Arrestin-mediated NOPR activation of ERK and JNK MAPKs. The results suggest that phosphorylation of NOPR at serine 363 by GRK3 acts to facilitate arrestin3 recruitment and receptor internalization, and that arrestin3 is required for NOPR activation of JNK signaling.

EXPERIMENTAL PROCEDURES

Chemicals

Nociceptin and Pertussis Toxin were purchased from R & D Systems (Bristol, UK). All drugs were dissolved in water unless otherwise indicated.

C-terminal Mutagenesis of NOPR-YFP

pcDNA3.1-NOPR-AY268428 (cDNA.org) was amplified using High fidelity *Taq* and the following primers to remove the stop codon. The PCR product was then digested and cloned into the 5′ EcoRI and 3′ XhoI sites of pcDNA3-YFP (Addgene Plasmid 13033). To create pcDNA3-NOPR-YFP: 5′EcoRI-NOPR-FWD, AGT GTG GTG GAA TTC ACC ATG GAG CCC, 3′-XhoI-NOPR-REV, TTG CTC ACC ATC TCG AGT CCT GCG GGC CGC GGT A. The cDNA was amplified with High fidelity *Taq* using the same 5′ EcoRI forward primer and one of the following 3′ Ultramer primers (IDT, Coralville, IA) to remove the stop codon and generate point mutants. The PCR product was then digested and cloned into the 5′ EcoRI and 3′ XhoI sites of pcDNA3-YFP (Addgene plasmid 13033). To create pcDNA3-NOPR S363A-YFP 3′XhoI-NOPR-REV, CTCTAGACTCGAGTCcTGCGGGCCGCGGTACCGTCTCAGcGGTCTTGCAGGCCAGGGCCAC; pcDNA3-NOPR T362/S363A-YFP (TS) 3′ XhoI-NOPR REV, CTCTAGACTCGAGTCcTGCGGGCCGCGGTACCGTCTCAGcGGcCTTGCAGGCCAGGGCCAC; pcDNA3NOPR T362/S363/T365A-YFP-(TST) 3′XhoI-NOPR REV, CTCTAGACTCGAGTCcTGCGGGCCGCGGTACCGgCTCAGcGGcCTTGCAGGCCAGGGCCAC; pcDNA3NOPR S337A/S346A/S351A-YFP(SSS)3′XhoI-NOPR-REV, CTCTAGACTCGAGTCcTGCGGGCCGCGGTACCGTCTCAGAGGTCTTGCAGGCCAGGGCCACGTCCTTGGCAATGgCGCGCACGCGGTCAGcCACCTGCACGTCCCGGCGCAGGGCAGcTGCACAGCAGAAC. All mutations were confirmed by DNA sequencing (AGCT Inc., Wheeling, IL).

Cell Culture and Transfection of NOPR-YFP Expressing HEK293 Cells

HEK293 cells were grown in Dulbecco's modified Eagle's media/F-12 media supplemented with 10% fetal bovine serum containing 1× penicillin/streptomycin (Invitrogen) and 400 μg/ml of G418 to maintain selective pressure in NOPR-YFP expressing cells. HEK293 cells expressing human NOPR-YFP and NOPR-YFP C-terminal mutants were generated as previously described (10). Briefly, stable HEK cell lines expressing pcDNA3 containing NOPR-YFP, NOPR-S337/346/351A, NOPR-T362/S363/T365A, NOPR-T362/S363A, and NOPR-S363A were generated by transfecting HEK293 cells with identical amounts of cDNA (5 μg) coding for each NOPR-type for 2–3 h using Superfect (Qiagen) reagent per the manufacturer's instructions and then placing the HEK293 cells under selective pressure with G418 (800 μg/ml) for 3 weeks. Colonies of surviving cells were selected and grown into individual 100-mm cell culture plates under 400 μg/ml of selective pressure for an additional 2–3 weeks. Cells were then FACS (Washington University FACS Sorting Facility) sorted for equal fluorescence between mutants and wild-type NOPR to further ensure equal receptor expression in each group. Sorted NOPR-YFP expressing HEK293 cells were then grown to confluence into larger T-75 flasks split and cryo-preserved for future use.

Calcium Channel Electrophysiology, Cell Culture, and Transfection

The coding region of human N-type Ca^{2+} channel $Ca_V2.2$ subunit was cloned into plasmid pIRES2-EGFP (Clontech), under the CMV promoter. Plasmids encoding mCherry-tagged NOPR receptor (4 μg) and $Ca_V2.2$ subunit (2 μg) were co-transfected into stable HEK293 cells expressing the Ca^{2+} channel auxiliary β_{1C} and $\alpha_2\delta$-1 subunits, using Lipofectamine 2000. One day post-transfection, cells were seeded on Matrigel-coated glass coverslips and recorded 24–48 h later.

Electrophysiology—Transfected cells were identified by EGFP and mCherry fluorescence. Whole cell patch clamp recordings were performed at room temperature with a MultiClamp 700B amplifier (Molecular Devices). pClamp 10 (Molecular Devices) software was used to acquire and analyze data. Cell capacitance and series resistance were constantly monitored throughout the recording. The recording chamber was perfused with extracellular solution (1 ml/min) containing (in mM): 130 NaCl, 2 KCl, 2 $CaCl_2$, 2 $MgCl_2$, 25 HEPES, 30 glucose, pH 7.3, with NaOH, 310 milliosmole. The pipette solution contained (in mM): 110 CsCl, 10 EGTA, 4 ATP-Mg, 0.3 GTP-Na, 25 HEPES, 10 Tris phosphocreatine, 20 units/ml of creatine phosphokinase, pH 7.3, with CsOH, 290 milliosmole. Recording pipettes had <3.5 MΩ resistance. Series resistance (<15 MΩ) was compensated by 80%. Current traces were corrected with on-line P/6 trace subtraction. Signals were filtered at 1 kHz and digitized at 10 kHz. Cells were held at −80 mV and depolarized from −80 to +10 mV for 40-ms pulses every 10 s. After establishing baseline recording, cells were perfused with 1 μM nociceptin while evoking Ca^{2+} currents via depolarizing pulses. In some experiments, transfected cells were incubated in culture medium containing 1 μM nociceptin at 37 °C for 30 min. Cells were then perfused with extracellular solution for 5 min to wash off nociceptin before conducting whole cell patch clamp recordings. Data were calculated as percent inhibition of calcium currents and plotted.

cAMP Assay—HEK293 cells were transiently co-transfected with pGloSensor-22F cAMP plasmid (Promega E2301) and NOPR-YFP or NOPR-S363A containing plasmids using JetPrime transfection reagent (Polyplus-transfection SA, Illkirch, France) per the manufacturer's instructions. Cells were transfected and plated on 96-well tissue culture-treated plates (Costar) and allowed to recover overnight at 37 °C, 5% CO_2. The next day, media was replaced with 2% GloSensor reagent (Promega) suspended in CO_2-independent growth medium (Invitrogen) and incubated at room temperature for 2 h. Baseline luminescence recordings were taken and cells were exposed to varying concentrations of nociceptin for 5–10 min before adding 10 μM forskolin. Luminescent readings were taken ~20 min post drug addition using a SynergyMx microplate reader (BioTek, Winooski VT). Relative luminescent units were normalized to the maximal response evoked by forskolin while in the presence of nociceptin. Subsequent concentration-response curves were fit using standard nonlinear regression to obtain IC_{50} values using GraphPad Prism (version 5.0d, GraphPad Software, San Diego CA). Triplicate data points were averaged per experiment. Data are expressed as mean ± S.E.

NOPR-YFP Immunocytochemistry (ICC) and Confocal Microscopy

NOPR-YFP and NOPR-YFP C-terminal mutants were grown on poly-D-lysine coverslips in 24-well plates and placed in a 37 °C 5% CO_2 incubator. Following drug treatment, cells were washed three times with PBS and then fixed in 4% paraformaldehyde for 20 min, washed in PBS 3 times, blocked for 2 h in 5% normal goat serum, 0.3% Triton X-100 in PBS (blocking buffer) at room temperature, and then incubated overnight with primary antibody in blocking buffer. The following primary antibody concentrations were used: goat anti-rabbit phospho-pJNK MAPK antibody (1:500, Cell Signaling, Beverly, MA) and anti-FLAG M2 antibody was used (1:1000, Sigma). Following primary antibody exposure and a 3 times wash in PBS, coverslips were exposed to secondary antibody, goat anti-rabbit Alexa Fluor 555 (1:1000, Molecular Probes, Eugene, OR) and goat anti-rabbit IgG 488 Alexa Fluor conjugate (1:400, Molecular Probes) diluted in blocking buffer and incubated with coverslips for 1 h at room temperature. Coverslips were mounted using VECTASHIELD (Vector Laboratories, Burlington, CA) and sealed with clear nail polish. Fluorescent YFP signals were excited at 488 nm, Alexa Fluor 555 fluorescent signals were excited at 543 nm detected and merged as appropriate. All imaging was performed within the Washington University Pain Center Confocal Imaging Center or the Washington University Bakewell Imaging Center. Images, cells, and treatment groups were chosen and analyzed in a blinded fashion. Fields of cells and 3–4 individual cells were chosen at random per coverslip, per treatment, in a triplicate fashion. Experimental "*n*" reflects an entirely new passage of cells and drug treatment set. Semi-quantitative analysis of internalization of NOPR-YFP and mutants was calculated as previously described using Metamorph analysis algorithm for pixel intensity measurements (19) of internalized fluorescence (*F*) measures. To determine internalized percentages, equal cell shapes and sizes were always chosen; concentric circles around the fluorescence, background internal fluorescence (untreated controls) or internalized (treated) portions of the entire cell were drawn in Metamorph, integrated pixel intensities were recorded for each using the Metamorph algorithm for integrating intensity and internalized receptors were calculated using Inside F/Total F × 100.

siRNA Transfection, Imaging, and qRT-PCR

The following shRNA constructs RFP CTCAGTTCCAGTACGGCTCCA; GRK3NM_005160CAGTAAATGCAGACACAGATA; GRK2NM_001619ATTATTGTGATTTCCCGTGGC; Arrestin2NM_004041GCCAGTAGATACCAATCTCAT; *pLKO1.0* (Washington University RNAi core facility) Arrestin3NM_004313 CTTCGTAGATCACCTGGACpLKO1.5 (SIGMA) were transfected and stably expressed under selective pressure with puromycin for 4–6 weeks to establish siRNA knock-out lines for GRK2, GRK3, ARR2, ARR3, in HEK293 cells. NOPR-YFP was then transiently transfected into each siRNA cell line. All siRNA transfections used JetPrime (Polyplus-transfection SA, Illkirch, France) per the manufacturer's instructions.

Confocal Imaging—Stable HEK293 cells expressing the five different shRNA constructs listed above were plated on 24-well plates with 12-mm poly-D-lysine-coated coverslips (BD Bioscience) containing 2 μg/ml of puromycin media at 50% confluence. Although cells are still in suspension, pcDNA3-NOPR-YFP was transiently transfected into cells using JetPrime per the manufacturer's instructions. 48 h after transfection cells were treated with 1 μM nociceptin at specified time points. Cells were immediately washed in cold PBS and quickly fixed in cold 4% paraformaldehyde for 15 min while gently rocking. Following the previously outlined ICC protocol, cells were imaged using a FV300 confocal microscope (Olympus) under a ×40 oil objective. Representative images were taken for RFP, GRK2, ARR2, GRK3, and ARR3 at different time points and analyzed using Metamorph. For immunoblot experiments stable HEK293 cells expressing the five different shRNA constructs listed above were plated on 24-well plates at 50% confluence in 2 μg/ml of puromycin media. Although cells are still in suspension pcDNA3-NOPR-YFP was transiently transfected into cells using JetPrime per the manufacturer's instructions. 48 h after transfection cells were treated with 1 μM nociceptin at specified time points.

qRT-PCR—Total RNA was isolated using the RNAgem Tissue Plus kit (Zygem) and One Step qRT-PCR was performed on a Applied Biosystems 7500 real time cycler using QuantiTect SYBR Green PCR kit and QuantiTect primers targeting human GAPDH, GRK2, ARR2, GRK3, and ARR3 (Qiagen). C_t values were collected in triplicate and relative $\Delta\Delta C_t$ were analyzed using REST 2009 software (Qiagen).

Immunoblotting—Western blots for phospho-MAPKs were performed as described previously (9). Briefly, NOPR-YFP and NOPR-S363A-YFP (NOPR-S363A) expressing HEK293 cells were cultured as described above. Cells were serum-starved a minimum of 4–6 h prior to drug treatment to avoid serum growth factor-induced MAPK activation. Cells were treated with drugs at various time points in cell culture medium at 37 °C and then lysed in 350 μl of lysis buffer containing 50 mM

Tris-HCl, 300 mM NaCl, 1 mM EDTA, 1 mM Na_3VO_4, 1 mM NaF, 10% glycerol, 1% Nonidet P-40, 1:100 of phosphatase inhibitor mixture set 1 (Calbiochem), and 1:100 of protease inhibitor mixture set 1 (Calbiochem). Lysates were sonicated for 20 s and then centrifuged for 15 min (14,000 × *g*, 4 °C), the pellet was discarded, and sample supernatants were stored at −20 °C. Protein concentration was determined by a Pierce BCA (Thermo Scientific) assay with bovine serum albumin as the standard. 20 μg of total protein was loaded onto nondenaturing 10% bisacrylamide precast gels (Invitrogen) and run at 150 V for 1.5 h. For determination of molecular weights prestained molecular weight ladders (Invitrogen) were loaded along with protein samples. Blots were transferred to nitrocellulose (Whatman, Middlesex, UK) for 1.5 h at 30 mV, blocked in TBS, 5% bovine serum albumin for 1 h, incubated overnight at 4 °C with a 1:1000 dilution of goat anti-rabbit phospho-pJNK MAPK antibody or goat anti-rabbit phospho-ERK 1/2 (Thr-202/Tyr-204) antibody (Cell Signaling) or mouse β-actin (1:5000, Abcam). Following overnight incubation, membranes were washed 4× for 15 min in TBST (Tris-buffered saline, 1% Tween 20) and then incubated with the IRDye™ 800- and 700-conjugated affinity purified anti-rabbit or anti-mouse IgG at a dilution of 1:20,000 in a 1:1 mixture of 5% milk/TBS and Li-Cor blocking buffer (Li-Cor Biosciences, Lincoln, NE) for 1 h at room temperature. Membranes were then washed 4× for 15 min in TBST, 1× for 10 min in TBS to remove Tween 20 (which can cause high background fluorescence on the Odyssey imaging system), and analyzed as described below.

Data Analysis

All Immunoblots were scanned using the Odyssey infrared imaging system (Li-Cor Biosciences). Band intensity was measured using Odyssey software following background subtraction and integrated band density in high-resolution pixels was calculated. For both pERK and pJNK blot quantitation, all subtypes of ERK (1 and 2) and pJNK (1, 2, 3) were quantified together, as there was no evidence using these epitope antibodies that JNK subtypes 1, 2, and 3 were differentially regulated by NOPR stimulation. All pERK/pJNK bands were normalized to β-actin, as an equal protein loading control. Data were then calculated to percentage of control or vehicle sample band intensity (basal, 100%) and plotted using GraphPad (GraphPad Prism 5.0) software. Concentration-response data were fit using nonlinear regression (Prism 5.0). Statistical significance was taken as $p < 0.05$, $p < 0.01$, or $p < 0.001$ as determined by the Student's *t* test or analysis of variance (ANOVA), followed by Dunnett's or Bonferroni post hoc tests where appropriate. Specific statistical tests and results are indicated in figure legends.

RESULTS

Serine 363 Is Required for Nociceptin-induced NOPR Internalization—Previous studies with μ-, κ-, and δ-opioid receptors have shown that C-terminal serines are crucial for mediating receptor desensitization and internalization (2). However, the key residue(s) involved in NOPR regulation have not been defined. Therefore, we generated mammalian expression constructs for YFP-tagged human NOPR and used site-directed mutagenesis to construct C-terminal NOPR-YFP serine/threonine to alanine mutants. Based on the highly conserved C-terminal cDNA sequence alignment between human, mouse, and rat (Fig. 1*A*) we began by mutating groups of putative serine/threonine amino acid residues and screening for changes in nociceptin-induced (1 μM) internalization (Fig. 1*B*). In HEK293 cells expressing NOPR-YFP, nociceptin caused a robust time-dependent receptor internalization peaking at 60–90 min following agonist treatment (Fig. 1, *B* and *C*).

Mutation of C-terminal serine 337, 346, and 351 had no effect on nociceptin-induced (1 μM, 60 min) NOPR internalization, with comparable internalization to the wild-type NOPR-YFP receptor (Fig. 1*D*). In contrast, mutation of the threonine 362, serine 363, threonine 365 sequence (TST) significantly blocked nociceptin-induced (1 μM, 60 min) NOPR-YFP internalization (Fig. 1*D*) as did mutation of only the threonine 362-serine 363 sequence. Finally, mutation of only serine 363 to alanine also caused a significant block of nociceptin-induced NOPR internalization (Fig. 1*E*) (**, $p < 0.01$ NOPR mutants *versus* NOPR-YFP, ANOVA, Dunnett's post hoc, $n = 4$ independent experiments performed in triplicate sets). Together, these data suggest that mutation of serine 363 to alanine in NOPR is sufficient to block the ability of the endogenous agonist of nociceptin to cause receptor internalization, and strongly implicate this residue as a crucial site for GRK phosphoregulation of NOPR.

Serine 363 Is Required for NOPR Desensitization—Previous reports have demonstrated that NOPR receptors couple to inhibition of N-type $Ca_V2.2$ calcium currents and readily desensitize in a time-dependent manner in sensory neurons (5, 6). To determine the pharmacological properties of NOPR and NOPR-S363A-mediated G-protein-mediated signaling and receptor desensitization, we measured the effects of nociceptin on NOPR-mediated cAMP inhibition and blockade of N-type $Ca_V2.2$ calcium currents in both NOPR-YFP and NOPR-S363A HEK293 cells. The $Ca_V2.2$ subunit of N-type calcium channels expressing the auxiliary β1C and α2δ-1 subunits were coexpressed with NOPR-YFP. We used patch clamp recording to measure whole cell Ca^{2+} currents through N-type channels. The transfected cell was held at −80 mV and depolarized to +10 mV for 40 ms to elicit inward current. Perfusion of 1 μM nociceptin resulted in similar and significant inhibition of whole cell Ca^{2+} currents in both NOPR-YFP and NOPR-S363A expressing HEK293 cells. Nociceptin induced comparable inhibition of Ca^{2+} currents as previously reported (Fig. 2, *A* and *B*) (5). In contrast, pretreatment of cells with 1 μM nociceptin (30 min, 37 °C) prior to recording caused robust and significant desensitization ($p < 0.001$, $n = 11$) of subsequent nociceptin-mediated inhibition of Ca^{2+} currents in NOPR-YFP expressing HEK cells (Fig. 2, *A* and *B*). However, in cells expressing NOPR-S363A, the same nociceptin pretreatment did not result in any subsequent desensitization of nociceptin-induced inhibition of Ca^{2+} currents (Fig. 2, *A* and *B*).

We next determined whether mutation of serine 363 would also impact NOPR-induced inhibition of cAMP. Both NOPR-YFP and NOPR-S363A inhibited cAMP with equal potency and efficacy, suggesting that C-terminal serine 363 is not required for G-protein coupling to adenylate cyclase inhibition (IC_{50} for

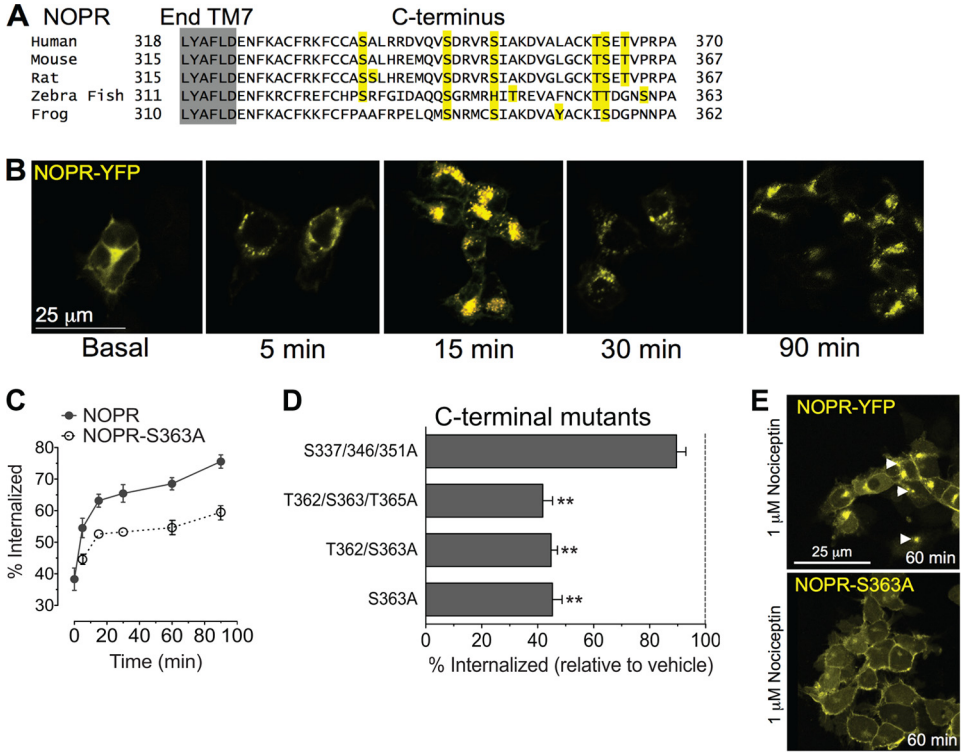

FIGURE 1. **Carboxyl-terminal serine and threonine residues in NOPR are required for receptor internalization.** *A*, C-terminal, amino acid sequence alignment of NOPR human, mouse, rat, zebrafish, and frog residues. *Gray shading* indicates end of transmembrane (*TM*) 7. *Yellow* highlighted residues represent putative phosphorylation, regulatory sites. *B*, representative time course of NOPR-YFP and NOPR-S363A expressing HEK293 cells following vehicle (basal) or NOPR-agonist (1 μM nociceptin) treatment at various time points ($n = 8$ independent experiments). *C*, mean ± S.E. data showing rate of NOPR-YFP internalization following nociceptin (1 μM) treatment ($n = 10$). *D*, relative NOPR-C-terminal mutant-YFP internalization as compared with wild-type NOPR internalization (*dashed line*) at the 60-min (1 μM nociceptin) time point. Data show that the serine 337, 346, and 351 (SSS) to alanine mutant internalizes in response to nociceptin treatment. In contrast, the threonine 362, serine 363, and threonine 365 (TST) to alanine mutant significantly attenuated nociceptin-induced NOPR internalization. Similar significant attenuation of NOPR-internalization was also present in the Thr-362, Ser-363 to alanine mutant, and S363 mutant alone, demonstrating a critical role of Ser-363 in regulation of NOPR (**, $p < 0.01$, one-way ANOVA, Dunnett's post hoc, mutants *versus* NOPR-YFP control, $n = 12$, in triplicate). *E*, representative confocal images of 1 μM nociceptin-treated (60 min) NOPR-YFP as compared with NOPR-S363A showing lack of agonist-induced internalization in NOPR-S363A ($n = 12$).

nociceptin-induced inhibition of cAMP at NOPR-YFP = 0.704 ± 0.12 nM, at NOPR-S363A = 0.69 ± 0.17 nM) (Fig. 3*C*). Treatment with 1 μM nociceptin resulted in similar and significant inhibition of cAMP in both NOPR-YFP and NOPR-S363A expressing cells (Fig. 3, *C* and *D*). In contrast, pretreatment of cells with 1 μM nociceptin (30 min, 37 °C) prior to a subsequent nociceptin (1 μM) challenge caused robust and significant desensitization ($p < 0.01$, $n = 4$–13) of nociceptin-mediated inhibition of cAMP in NOPR-YFP expressing cells (Fig. 3*D*). However, in cells expressing NOPR-S363A, the same nociceptin pretreatment did not result in any subsequent desensitization of nociceptin-induced inhibition of cAMP (Fig. 3*D*) ($n = 4$–13, $p < 0.05$). Taken together, these data suggest that mutation of serine 363 to alanine prevents NOPR-mediated desensitization to both G-protein α (cAMP) and $\beta\gamma$ subunit (Ca^{2+} channel) signaling, and further support the conclusion that serine 363 is a crucial C-terminal residue involved in the functional regulation of NOPR.

Nociceptin-induced NOPR Internalization Requires GRK3/Arrestin3—Phosphorylation of C-terminal serines by GRKs, subsequent arrestin binding, and endocytosis are well established mechanisms for opioid-receptor regulation. In particular, ligand-induced regulation of opioid receptors typically involves GRK2, GRK3, and Arrestin2/Arrestin3. (10, 20). Using small interfering siRNA in HEK293 cells expressing NOPR-YFP, we selectively knocked down the individual GRKs 2 and 3, and Arrestin2 and -3 (also called β-arrestin1 and β-arrestin2) and determined which GRK and arrestin are required for NOPR internalization.

To assess the role of GRKs in NOPR internalization we knocked down expression of GRK2 and GRK3 and examined nociceptin-induced internalization of NOPR (1 μM, 60 min). Nociceptin caused significant NOPR-YFP internalization ($n = 3$, $p < 0.05$) in GRK2 siRNA expressing cells, but not in cells expressing GRK3 siRNA (Fig. 3, *A* and *B*). We used quantitative RT-PCR (qRT-PCR) of mRNA for GRK2 and GRK3 to confirm significant (>50%, $p < 0.001$) knockdown of mRNA for each kinase (Fig. 3*C*). We next determined the effect on NOPR internalization by using siRNA to knockdown arrestin2 and arrestin3. Nociceptin (1 μM, 60 min) caused significant internalization ($n = 3$, $p < 0.05$) in Arrestin2 siRNA expressing cells, but not in cells expressing Arrestin3 siRNA (Fig. 3, *D* and *E*). Again, we used qRT-PCR of mRNA for arrestin2 and arrestin3 to confirm significant (>50%, $p < 0.001$) knockdown of expression for each arrestin subtype (Fig. 3*C*). Control siRNA (off target) transfected cells showed normal internalization of NOPR-YFP following agonist treatment, further confirming the selectivity of our GRK and arrestin siRNA knockdown approach (Fig. 3*F*).

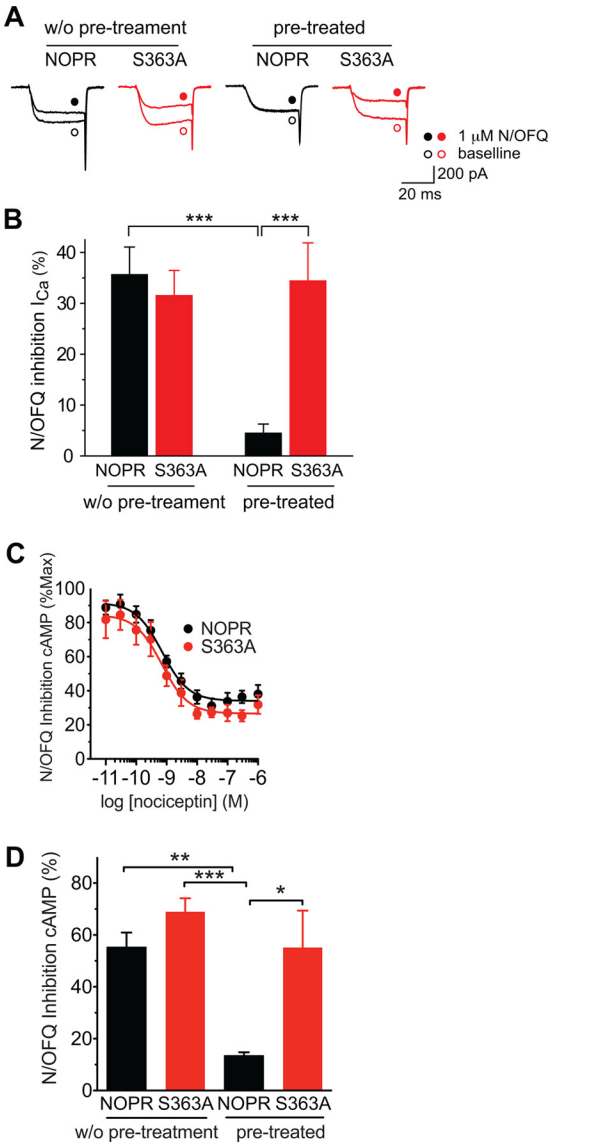

FIGURE 2. **Serine 363 in NOPR is required for agonist-induced receptor desensitization of coupling to N-type Ca^{2+} channels and inhibition of cAMP.** *A,* representative N-type Ca^{2+} current traces in response to square pulse depolarization (from −80 to +10 mV for 40 ms) before and after 1 μM nociceptin application in the exemplar cell from each experimental group. *B,* percentage of nociceptin-induced inhibition of Ca^{2+} current (I_{Ca}) in cells expressing wild-type NOPR or the S363A mutant, with or without pre-treatment of 1 μM nociceptin at 37 °C for 30 min, respectively (n = 8–10 cells in each group, ***, $p < 0.001$, two-way ANOVA with post hoc Bonferroni test). *C,* concentration-response curves for nociceptin-induced inhibition of cAMP in NOPR-YFP (*black*) and NOPR-S363A expressing HEK293 cells (*red*) (n = 5–10). IC_{50} for nociceptin-induced inhibition of cAMP at NOPR = 0.704 ± 0.12 nM, at NOPR-S363A = 0.69 ± 0.17 nM. *D,* percentage of nociceptin-induced inhibition of cAMP in cells expressing wild-type NOPR or the S363A mutant, with or without pretreatment of 1 μM nociceptin at 37 °C for 30 min, respectively (n = 4–13, *, $p < 0.05$; **, $p < 0.01$; ***, $p < 0.001$, two-way ANOVA with post hoc Bonferroni test).

Together, these data suggest that NOPR internalization requires GRK3 and arrestin3.

Nociceptin Induces Arrestin3 but Not Arrestin2 Membrane Translocation—We also examined whether nociceptin could preferentially induce membrane translocation of arrestin3 to further establish selective interaction of the nociceptin-engaged NOPR with the arrestin3 isoform. In NOPR-YFP expressing cells transfected with FLAG-arrestin3, arrestin3 distribution is diffuse and cytosolic in untreated cells (Fig. 4*A*), but labeling becomes punctate and increasingly at the membrane after nociceptin treatment (1 μM, 15, 30 min, n = 3), indicative of specific recruitment to the membrane (Fig. 4*A*); whereas in NOPR-YFP cells transfected with FLAG-arrestin2, nociceptin failed to induce a shift in localization of arrestin2 to the membrane (1 μM, 15, 30 min, n = 3). Furthermore, in cells expressing NOPR-S363A and FLAG-Arrestin3 show a similar lack of significant membrane translocation of FLAG-Arrestin3 following nociceptin treatment at any time point (Fig. 4) (n = 3).

We also utilized a novel arrestin3 mutant recently characterized as deficient in binding to both activated and inactive receptors to determine whether we could visualize its stable translocation at the cell membrane. This FLAG-arrestin3-KNC has 2 key phosphate-binding lysines and 10 residues that engage receptor elements all mutated to alanines (15). Interestingly, in cells transfected with both NOPR-YFP and FLAG-arrestin3-KNC, nociceptin treatment (1 μM, 15, 30 min, n = 3) did not promote translocation from the cytosol to the membrane of this FLAG-arrestin3-KNC, suggesting that binding of arrestin3 to NOPR may in part stabilize the arrestin3 at the membrane (Fig. 4 C). Together, these data suggest that arrestin3 translocates to the membrane in NOPR cells in response to agonist and further supports arrestin3 as a key isoform in nociceptin-induced NOPR regulation.

NOPR Serine 363 to Alanine Mutation Prevents Biphasic Nociceptin-induced c-Jun N-terminal Kinase Phosphorylation (pJNK)—Recent studies have shown that GPCRs activate non-canonical signaling pathways including MAPK cascades in both G-protein-dependent and -independent manners in biphasic patterns (10, 13, 21, 22). Treatment of cells expressing NOPR-YFP with the selective NOPR agonist nociceptin caused a time- and concentration-dependent increase in pJNK (Fig. 5, *A*, *C*, and *G*) that was completely absent in untransfected control HEK293s (data not shown, n = 3). However, HEK293 cells expressing mutant NOPR-S363A did not show a concentration-dependent increase in pJNK at 15 min and onward at time points following nociceptin treatment (Fig. 5, *B*, *C*, and *G*). The differences in response were not due to differences in expression (see "Experimental Procedures") because NOPR-YFP and NOPR-S363A HEK293 cells were generated to express equal levels of receptor using FACS sorting of equal surface fluorescence. Surprisingly, both NOPR-YFP and NOPR-S363A show equivalent nociceptin-induced ERK1/2 phosphorylation (pERK) in time- and concentration-dependent manners (Fig. 5, *D*, *E*, *F*, and *H*) and equal potency and efficacy in cAMP inhibition. In addition, ERK and pJNK were activated with similar potency and kinetics in NOPR (non-YFP tagged) expressing HEK cells suggesting that the C-terminal YFP tag does not interfere with signaling of the receptor through these pathways (data not shown).

Dominant-Positive Arrestin3, but Not Arrestin2 Rescues NOPR-S363A-mediated pJNK and Receptor Internalization—To assess whether NOPR-S363A fails to activate JNK because agonist-bound NOPR-S363A is unable to recruit arrestin and internalize as effectively as NOPR-YFP, we transfected the dominant-positive forms of arrestin3-FLAG (DP-Arr3) and arrestin2-FLAG (DP-Arr2) into NOPR-S363A HEK293 cells. This form of arrestin has

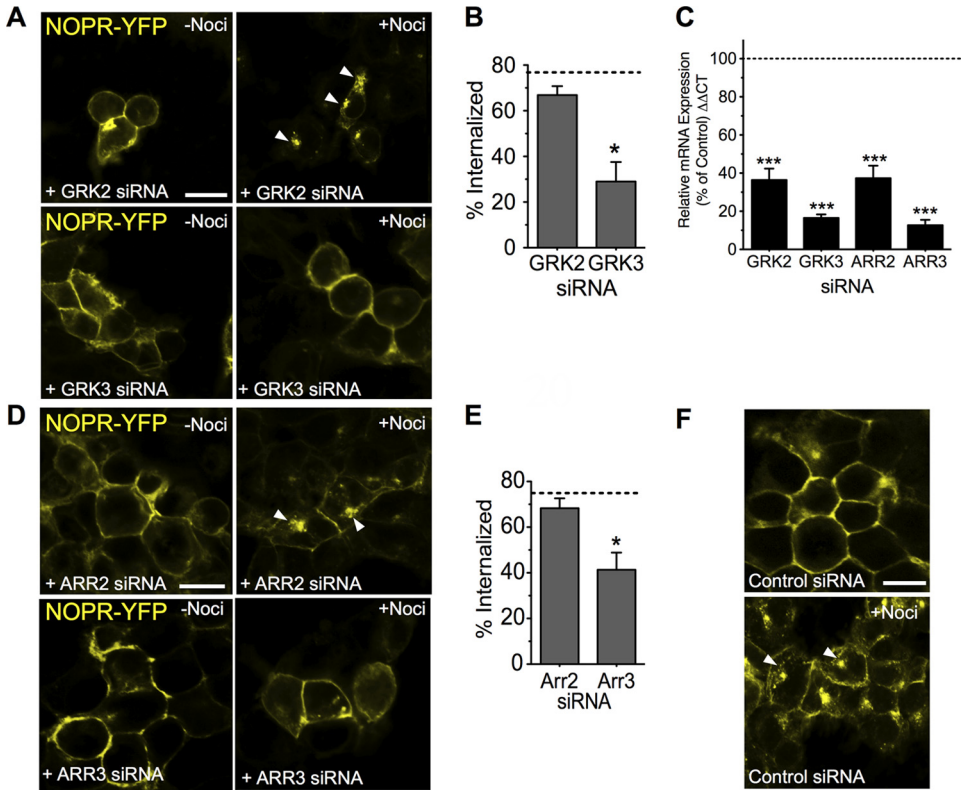

FIGURE 3. **siRNA knockdown of GRK3 and arrestin3 prevent nociceptin-induced NOPR internalization.** *A,* representative confocal images of NOPR-YFP expressing HEK293 cells in the presence of siRNA for GRK2 and GRK3 in the absence and presence of 1 μM nociceptin (−*noci*, +*noci*, respectively, 1 h treatment) ($n = 3$). *Scale bar* = 20 μm. *B,* quantitation of nociceptin-induced NOPR-YFP internalization in GRK2 and GRK3 siRNA knockdown in HEK293 cells ($p < 0.05$, *t* test, $n = 3$, in triplicate). *C,* qRT-PCR data of each mRNA as a percent relative to the control siRNA group. Data show mean siRNA knockdown results ± S.E. (using $2\Delta\Delta C_t$ method) following various siRNA transfections and confirm significant knockdown of mRNA for GRK2, GRK3, arrestin2 (*Arr2*), and arrestin3 (*Arr3*) ($n = 3$, one-way, ANOVA, ***, $p < 0.001$ Dunnett's post hoc *versus* control). *D,* representative confocal images of NOPR-YFP expressing HEK293 cells in the presence of siRNA for arrestin2 and arrestin3 in the absence and presence of 1 μM nociceptin (−*noci*, +*noci*, respectively, 1 h) ($n = 3$). *Scale bar* = 20 μm. *E,* quantitation of nociceptin-induced NOPR-YFP internalization in arrestin2 and arrestin3 siRNA knockdown HEK293 cells ($n = 3$, in triplicate). *F,* representative confocal images of control siRNA (off target) transfected NOPR-YFP cells before and after nociceptin treatment confirming that internalization block by GRK3/Arrestin3 siRNA is not due to nonspecific cellular effects ($n = 3$). *Scale bar* = 20 μm.

been previously demonstrated to be constitutively active and can bind to agonist-bound receptors independent of receptor phosphorylation (23–27).

In NOPR-S363A expressing cells transfected with DP-Arr3 and then stimulated with 1 μM nociceptin, the NOPR-S363A receptor was able to internalize and cause activation of pJNK (Fig. 6, *A–D*) in a similar fashion to NOPR-YFP receptors treated with nociceptin (1 μM, 30 min, $n = 3$). Successful transient transfection of DP-Arr3 was confirmed by increased FLAG immunolabeling in NOPR-S363A cells (~20–30% of total HEK population). In contrast, transfection of DP-Arr2 into NOPR-S363A expressing cells failed to rescue internalization ($n = 3$). In addition, control transfection of wild-type arrestin3 failed to induce a significant increase in NOPR-S363A activation of pJNK following nociceptin treatment (Fig. 6, *B* and *D*).

The effect of the DP-Arr3 transfection on NOPR-S363A-mediated pJNK 1/2/3 activation was also quantified using immunoblotting. We found that transfection of DP-Arr3 activation following treatment with nociceptin significantly (*, $p < 0.05$, test, $n = 4–6$) restored late phase NOPR-S363A-mediated JNK signaling (Fig. 6*B*). Taken together, these results suggest that serine 363 phosphorylation and the subsequent recruitment of arrestin are required for maximal NOPR-YFP internalization and activation of pJNK.

NOPR-induced pJNK Requires Both $G\alpha_i$-protein-dependent and -Independent Arrestin3 Pathways—Because we found a biphasic phosphorylation profile for NOPR-induced JNK activation (Fig. 4) we determined if each phase was either G-protein or arrestin dependent. We found that treatment with pertussis toxin, an inhibitor of $G\alpha_i$ signaling via ADP-ribosylation (300 ng/ml, 18 h) significantly blocked ($p < 0.05$) nociceptin-induced pJNK (1 μM) at the 5-min time point in both NOPR-YFP and NOPR-S363A expressing cells (Fig. 7, *A* and *B*) ($n = 6–11$). These data suggest that the early phase of NOPR-mediated JNK signaling requires $G\alpha_i$.

We next examined the second phase of NOPR pJNK signaling using siRNA knockdown of GRK2, GRK3, arrestin2, and arrestin3. Interestingly, we found that late phase (30 min) nociceptin-induced pJNK required GRK3 and arrestin3, but not GRK2 and arrestin2, because knockdown of GRK3 and arrestin3 significantly attenuated ($p < 0.05$) nociceptin-induced pJNK activation in NOPR-YFP expressing cells (Fig. 7, *C* and *D*). In addition, transfection of control siRNA had no effect on nociceptin-induced pJNK (Fig. 7, *C* and *D*). Together, these data suggest that GRK3 and arrestin3 are required for late phase nociceptin-induced pJNK activation, and further highlight the biphasic, bimodal nature of NOPR regulation and kinase signaling.

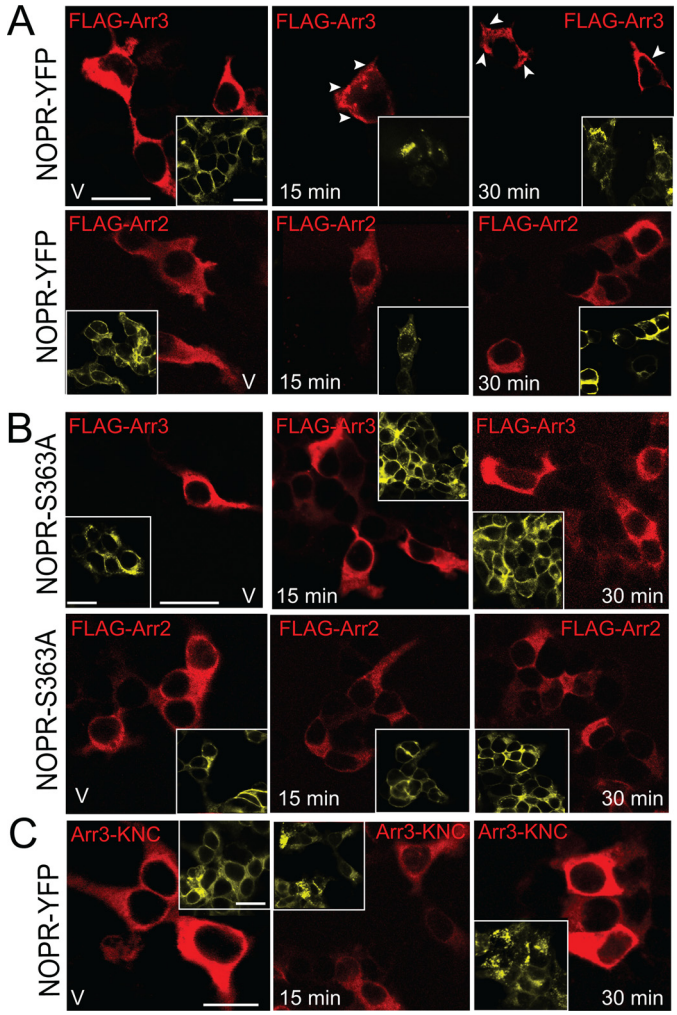

FIGURE 4. **Nociceptin induces membrane translocation of Arrestin3 but not Arrestin2.** *A,* representative confocal images of NOPR-YFP expressing HEK293 cells in the presence of FLAG-tagged arrestin3 (*Arr3*) or arrestin2 (*Arr2*) (*red channel*) in the absence (*V*, vehicle) or presence of 1 μM nociceptin at various time points ($n = 3$). *Scale bar* = 25 μm. *Inset* shows NOPR-YFP receptor internalization. *Arrows* indicate areas of membrane puncta indicative of arrestin3 translocation from cytosol toward membrane compartments. *Scale bar* = 20 μm. *B,* representative confocal images of NOPR-S363A expressing HEK293 cells in the presence of FLAG-tagged arrestin3 or arrestin2 (*red channel*) in the absence (*V*) or presence of 1 μM nociceptin at various time points ($n = 3$). *Scale bar* = 25 μm. *Inset* shows NOPR-S363A receptor (*yellow channel*). No significant evidence of translocation was found. *Scale bar* = 20 μm. *C,* representative confocal images of NOPR-YFP expressing HEK293 cells in the presence of FLAG-tagged arrestin3 KNC receptor binding deficient mutant in the absence (*V*, vehicle) or presence of 1 μM nociceptin at various time points ($n = 3$). *Scale bar* = 20 μm. *Insets* show NOPR-YFP receptor (*yellow channel*). No significant evidence of translocation was found. *Scale bar* = 20 μm.

DISCUSSION

The principle finding in this study was that NOP receptors are dynamically regulated through interactions at their carboxyl-terminal serine 363. Mutation of serine 363 to alanine prevented agonist-induced internalization, desensitization, and NOPR-mediated arrestin-dependent JNK MAPK signaling. Preincubation with nociceptin caused homologous NOPR desensitization of inhibitory cAMP signaling and Ca^{2+} channel inhibition. This homologous desensitization was absent in NOPR-S363A mutant receptor expressing cells. We also found that siRNA knockdown of GRK3 and arrestin3 prevented nociceptin-induced NOPR-YFP internalization. Additionally, we show that NOPR-induced JNK phosphorylation requires serine 363, GRK3, and arrestin3. These findings suggest that NOPR activation of pJNK may require GRK3 phosphorylation of serine 363 in the carboxyl-terminal domain of NOPR and ensuing association with the scaffold protein arrestin3. This proposed model (Fig. 8) is consistent with previous data suggesting that arrestin binding to GPCRs may enable MAPK activation, and acts to regulate receptor function (10, 20, 22).

Agonist-induced receptor desensitization is a primary mechanism for the subsequent internalization and down-regulation of opioid receptor G-protein signaling (2, 28, 29). In many cases, one crucial distal end carboxyl-terminal serine residue is required for regulation of μ-, κ-, and δ-opioid receptor function. Here we show in a similar fashion, that serine 363 is a crucial amino acid within NOPR necessary for both agonist-induced receptor internalization and homologous desensitization. We found that agonist-induced NOPR-YFP internalization peaked within 30 min, and that 30-min pretreatment of nociceptin prevents subsequent NOPR-mediated cAMP inhibition, as well as N-type $Ca_V2.2$ channel inhibition. This desensitization is consistent with the recently reported, nociceptin-induced loss of NOPR-mediated N-type $Ca_V2.2$ channel inhibition in populations of sensory neurons (6). Our data provide novel information as to the specific GRK and arrestin likely to mediate these effects. However, further study in similar types of NOPR-expressing neuronal cultures and *in vivo* studies will be necessary to fully validate the NOPR regulatory properties we defined here.

We did not directly measure the ligand-induced phosphorylation state of NOPR nor did we directly assess the kinetics of the putative nociceptin-induced GRK3-mediated receptor phosphorylation; however, given our mutagenesis results, we now have a more complete picture of the key amino acid epitope likely to be important for NOPR regulation and phosphorylation. Additionally, knowing that serine 363 is necessary for NOPR regulation we are now equipped to generate phospho-selective C-terminal NOPR antibodies for discerning NOPR regulation in endogenous neuronal systems, as have been used for both μ- and κ-opioid receptors (29–31). It is also important to note that the correlation between agonist-induced receptor phosphorylation, internalization, and desensitization is not always a direct relationship due to differences in ligand-receptor interactions and cell type. Thus, it will be necessary in future studies to fully characterize the kinetics of NOPR phosphorylation as they relate to the data in this study, and other reports, suggesting that rapid nociceptin-induced NOPR internalization is possible (Fig. 1*B*) (7).

Identifying the regulatory and desensitization mechanisms of NOPR will allow for a better understanding of how the NOP receptor communicates with N-type calcium channels *in vivo*, and how NOPR function is regulated following repeated nociceptin exposure. The specific mechanisms of NOPR regulation of N-type Ca^{2+} channel function remains an active debate (5, 6), although it is agreed upon by both groups that NOPR activation produces a 40% reduction in N-type Ca^{2+} currents. (5, 32). Our data in the present study corroborate these results and extend them by showing that NOPR serine 363 is an important player in desensitization of this $G\beta\gamma$-mediated signaling path-

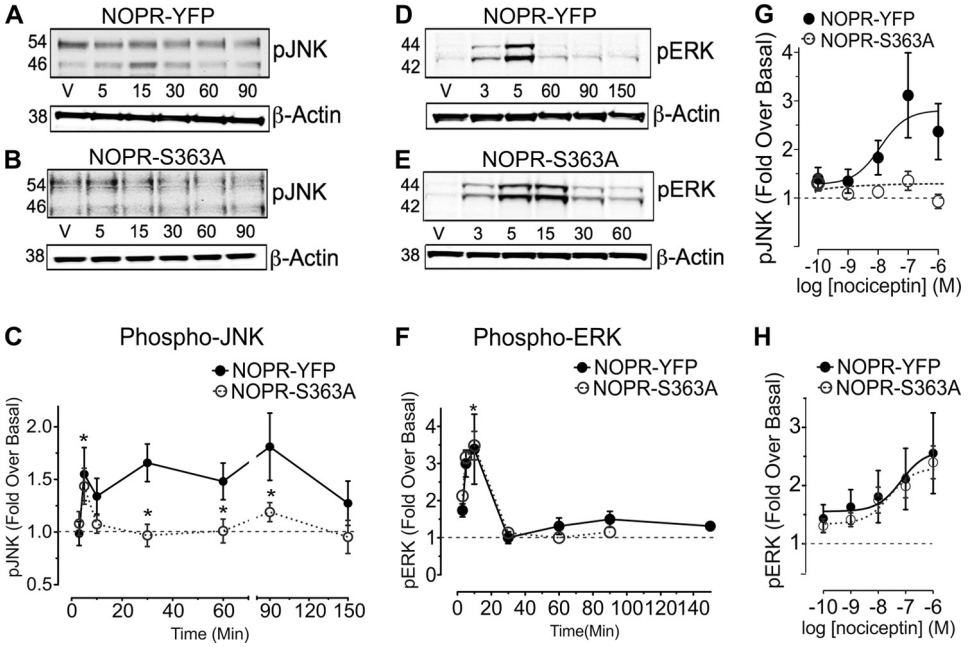

FIGURE 5. **NOPR-mediated pJNK activation requires serine 363.** *A–C,* HEK293 cells expressing either NOPR-YFP or NOPR-S363A treated with 1 μM nociceptin for different times at 37 °C and then resolved by Western blot. *A*, representative Western blot data for phospho-JNK MAPK (pJNK) and β-actin protein loading control in NOPR-YFP-expressing HEK cells. *B*, representative Western blot data for pJNK and β-actin protein loading in NOPR-S363A expressing HEK cells. *C*, the mean band intensities expressed as a percentage of basal-untreated control ± S.E. of NOPR-YFP (*filled circles*) and NOPR-S363A (*open circles*) mediated pJNK MAPK phosphorylation. pJNK levels significantly (*) increased at the 5-min post-nociceptin (1 μM) time point for both wild-type NOPR and mutant S363A. However, at the 15–90-min time points NOPR-S363A was unable to activate pJNK in response to nociceptin treatment as compared with the wild-NOPR-YFP ($n = 8$, where each n represents an independent experiment in duplicate, *, $p < 0.05$ using Student's t test). *D*, representative Western blot data for phospho-ERK1/2 (*pERK 1/2*) and β-actin protein loading control in NOPR-YFP-expressing HEK cells. *E*, representative Western blot data for phospho-ERK1/2 MAPK and β-actin protein loading control in NOPR-S363A-expressing HEK293 cells. *F*, mean band intensities expressed as a percentage of basal-untreated control ± S.E. of NOPR-YFP (*closed circles*) and NOPR-S363A (*open circles*) mediated ERK1/2 phosphorylation show a similar increase in the relative nociceptin-stimulated ERK1/2 activation, $n = 6$, where each n represents an independent experiment. *, $p < 0.05$ using the Student's t test. *G,* concentration-response curves of nociceptin-induced (30-min time point) NOPR-YFP (*closed circles*) *versus* NOPR-S363A-YFP (*open circles*), demonstrating that lack of agonist-induced pJNK in S363A is not due to a shift in the potency of nociceptin at activating pJNK (nociceptin, NOPR-YFP pJNK, $EC_{50} = 1.08$ nM ± 1.78; $n = 6$). *H,* concentration-response curves of nociceptin-induced (5 min time point) NOPR-YFP *versus* NOPR-S363A-YFP demonstrating equal agonist-induced pERK at both receptors (nociceptin, pERK, NOPR-YFP, $EC_{50} = 60$ nM ± 11 nM; NOPR-S363A, $EC_{50} = 24$ nM ± 0.5; $n = 6$).

way. Additionally, we found that NOPR-mediated $G\alpha_i$ signaling to cAMP is dynamically regulated via this same serine 363. Given that NOPR receptors have been implicated in stress signaling, pain, and affective behavior, our molecular analysis should provide some foundation for further studies exploring endogenous nociceptin-NOPR activity and down-regulation *in vivo*.

Activation of MAPK signal transduction by GPCRs has been demonstrated for numerous GPCR classes and ligand types, in a wide variety of cell lines and endogenous systems (22, 33–36). NOPR-mediated MAPK activation has not been examined in detail, although evidence does suggest that NOPR can activate ERK and p38 signaling (37, 38). There is some evidence for this NOPR-mediated MAPK signaling to involve PKA and PKC, although future work has not followed up on these data. Evidence for NOPR-induced JNK activation has also been reported, with interesting data suggesting that NOPR may activate JNK via multiple mechanisms including pertussis toxin-sensitive and -insensitive G-proteins, reminiscent of κ-opioid-mediated pJNK signaling (39, 40). Our results corroborate these data, showing similar nociceptin-induced pJNK kinetics and pertussis toxin sensitivity for early phase NOPR-mediated pJNK activation. However, we extend these findings and report that late phase NOPR-mediated pJNK requires GRK3 and arrestin3, suggesting that serine 363 is necessary for recruitment of this alternative NOPR-pJNK complex. Future studies will need to determine the additional proteins within this network, as well as the various microdomain differences between G-protein-dependent and -independent NOPR-induced JNK activation.

The function of arrestin in regulating opioid receptor desensitization, endocytosis, and phosphorylation is well established for the 3 original opioid receptor types (2). More recently, reports have shown that arrestins are necessary for ligand-directed signaling and functional selectivity at opioid receptors, and that they mediate vital opioid receptor-dependent behavioral effects (12, 20, 41). Our findings here suggest that NOPR shares some of these properties because we found siRNA knockdown of arrestin3 prevented NOPR-mediated pJNK. Dominant-positive arrestins have previously been reported to bind to the agonist-occupied receptor and mediate desensitization in the absence of receptor phosphorylation providing a useful tool for assessing the requirement of arrestin in signal transduction (10, 23). In these reports, δ- and κ-opioid receptor phosphorylation-insensitive C-terminal mutants were internalized and desensitized in a similar way as wild-type when these dominant-positive arrestins were co-expressed. Using NOPR-S363A-YFP co-transfected with a dominant-positive form of arrestin3 (Fig. 6*A*), we found that nociceptin was able to cause internalization of NOPR-S363A and also cause activation

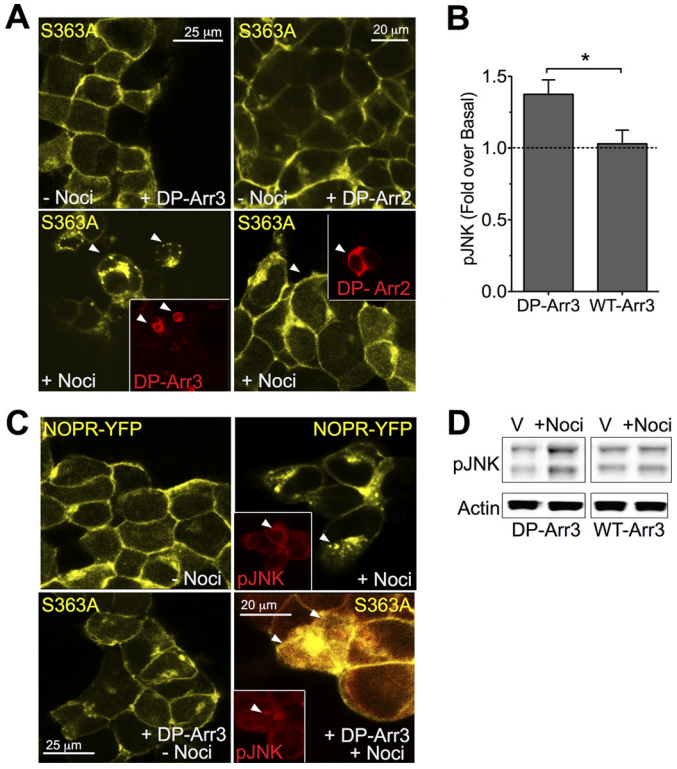

FIGURE 6. **DP-Arr3 rescues NOPR-S363A internalization and late phase pJNK.** HEK293 cells expressing NOPR-YFP or NOPR-S363A were fixed and labeled with anti-pJNK MAPK (*red*) or FLAG (*red*) and *yellow* fluorescence is the YFP signal corresponding to the each receptor (*A* and *C*). *A, upper left*, NOPR-S363A in the absence of nociceptin treatment (vehicle), expressing DP-Arr3. *Upper right*, NOPR-S363A in the absence of nociceptin treatment (vehicle), expressing DP-Arr2. *Lower left*, NOPR-S363A in the presence of nociceptin treatment (1 μM, 30 min), expressing DP-Arr3 showing restoration of NOPR-internalization. *Lower right*, NOPR-S363A in the presence of nociceptin treatment (1 μM, 30 min), expressing DP-Arr2 showing no rescue of NOPR internalization. *Red insets* show FLAG-Arr3 or FLAG-Arr2 immunofluorescence confirming expression of dominant-positive arrestin (30% transient transfection efficiency). *B,* mean ± S.E. of NOPR-S363A cells expressing dominant-positive arrestin3 (DP-Arr3) or overexpressing wild-type arrestin3 treated with vehicle or 1 μM nociceptin (30 min). Transient transfection of DP-Arr3 significantly rescued pJNK activity in NOPR-S363A ($n = 4–6$, $p < 0.05$, *t* test). *C, upper left*, NOPR-YFP in the absence of nociceptin treatment (vehicle). *Upper right*, NOPR-YFP in the presence of nociceptin treatment (1 μM, 30 min), showing NOPR internalization and pJNK immunoreactivity (pJNK-ir). *Lower left*, NOPR-S363A in the absence of nociceptin treatment (vehicle); *lower right*, NOPR-S363A in the presence of nociceptin treatment (1 μM, 30 min), expressing DP-Arr3 showing rescue of NOPR-induced pJNK-ir. Vehicle groups show no evident pJNK-IR staining over background, so the empty box is not shown. (All experiments were performed on 2–4 independent experiments in duplicate.) *D,* representative pJNK and actin loading control Western blots from cells expressing NOPR-S363A treated with nociceptin or vehicle (water) in cells coexpressing DP-Arr3 or Arr3.

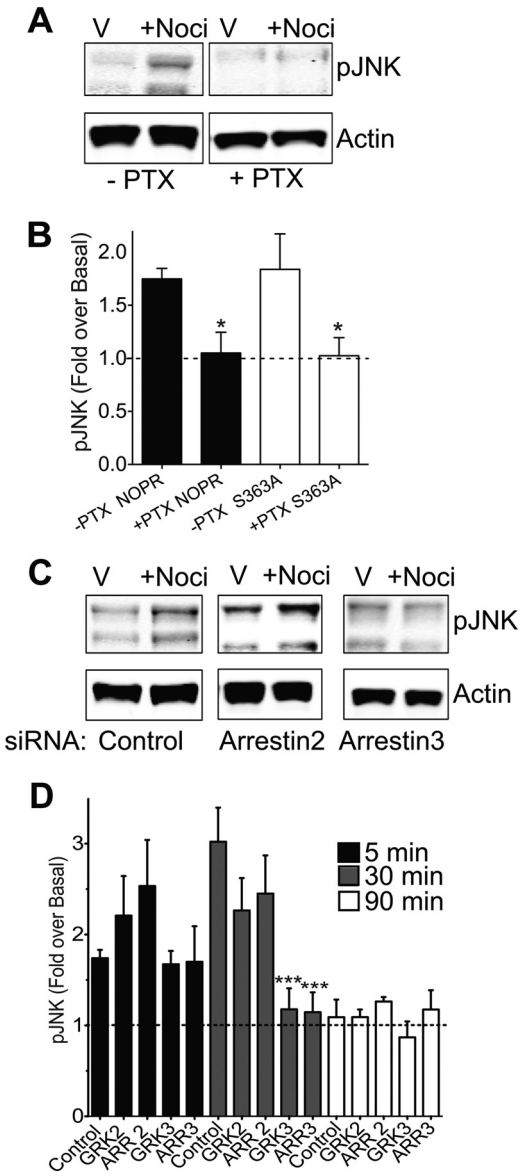

FIGURE 7. **Nociceptin-induced pJNK is both Gα_i-dependent and requires arrestin3.** *A, top*, representative Western blots of nociceptin (*noci*) induced pJNK (1 μM, 5 min) in NOPR-YFP expressing cells in the absence and presence of pertussis toxin (*PTX*) pretreatment (300 ng/ml, 18 h). *Bottom*, β-actin (actin) loading control confirming equal protein loading in each sample. *B,* nociceptin-induced pJNK ± S.E. data of NOPR-YFP and NOPR-S363A-mediated pJNK in the presence and absence of PTX ($n = 6–11$, $p < 0.05$, *t* test). *C,* representative Western blots of nociceptin-induced pJNK (1 μM, 30 min) in NOPR-YFP or NOPR-S363A co-expressed with control siRNA or siRNA for arrestin2 or arrestin3. Western blots show increased nociceptin-induced pJNK in control and arrestin2 knockdown, but no increase in pJNK in arrestin3 knockdown. *Bottom*, β-actin (actin) loading control confirming equal protein loading in each sample. *D,* nociceptin-induced pJNK ± S.E. data of NOPR-YFP-mediated pJNK in the presence and absence of various siRNAs including control, GRK2, GRK3, arrestin2, and arrestin3 ($n = 5$, ***, $p < 0.001$).

of JNK. These data support the concept that NOPR-mediated JNK activation requires arrestin. Interestingly, a recent report has suggested that certain JNK isoforms (JNK3) can become activated via arrestin scaffolding in the absence of receptor (16). Understanding the biochemical properties of NOPR-induced phosphorylation of specific JNK isoforms will also be a key next step.

Arrestin-mediated receptor endocytosis has been described for several GPCR classes, the rate of which depends on ligand, receptor, and cell type. Here we showed that NOPR internalization requires arrestin3 when the receptor is stimulated by nociceptin. However, it is important to note that arrestin2 may also interact with NOPR under different circumstances, including via other NOPR-selective agonists, or cell systems. The effects of GPCR functional selectivity are now widely reported, and our findings here open tantalizing possibilities for ligand bias at NOPR. Similarly, we identified a critical role for GRK3 and not GRK2 in NOPR endocytosis using siRNA technology. Although we did achieve significant knockdown of GRK2 and arrestin2 mRNA we cannot completely achieve full mRNA knockdown of each using this technology, so it is also plausible

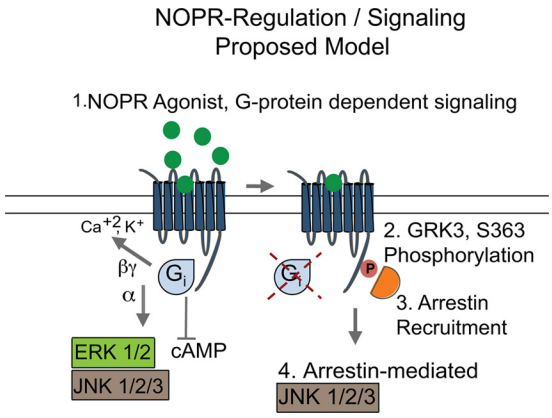

FIGURE 8. **Proposed model of NOPR regulation and G-protein/arrestin signal transduction.** *1,* agonist binds receptor and $G\alpha_i$ signaling commences. This includes $\beta\gamma$-mediated regulation of N-type calcium channels and $G\alpha$ signaling to inhibit cyclic AMP, activate ERK, and JNK. *2,* continued occupation of the receptor by agonist results in serine 363 phosphorylation, likely triggering additional phosphorylation events in the C terminus. *3,* Arrestin3 is recruited to the receptor ultimately causing receptor internalization by likely (although not yet defined) interactions with endocytosis machinery. *4,* Arrestin recruitment of JNK signal transduction. Future work will need to define the protein networks, and cellular mechanisms of NOPR-mediated ERK/JNK signaling *versus* arrestin-mediated pJNK activity.

that residual expression may still play a role in NOPR regulation. Furthermore, we cannot completely rule out a role for GRK2 in regulation of NOPR when exposed to different ligands or in other cell types expressing different ratios of regulatory proteins. This ligand-dependent GRK subtype recruitment is consistent with some very recent studies examining μ-opioid and β-adrenergic receptor function (42, 43). Additionally, arrestin scaffolding of the endocytic machinery is also well established. It is known that arrestin-clathrin interactions and Rab-GTPases are critical for these effects (44). Understanding how the NOPR-arrestin binding complex interacts with endocytic machine, and the kinetics of receptor degradation-recycling will be interesting avenues of further investigation.

The JNK MAPK pathway has been demonstrated to play a major role in environmental stress, inflammation, and cytokine pathway activation (45). JNK pathway activation has been recently shown to be involved in neuropathic pain responses in mice (46), and is well established to play a critical role in neurodegenerative disease progression (47). Both pathologies have also been linked to NOPR receptors in various contexts (48, 49) suggesting that NOPR-mediated pJNK signaling could have important *in vivo* implications; however, conclusions based from transfected cells are limited, and overexpression studies may force signal transduction that is not evident physiologically. Regardless, our results presented here are internally consistent and the behavioral *in vivo* implications of this process will require new investigations.

The NOPR crystal structure was just recently solved using an antagonist peptide mimetic (compound-24) bound to the NOPR receptor (50). This important study carefully models the NOPR ligand binding pocket and the critical amino acid residues required for high affinity NOPR binding. This recent discovery taken together with our results showing the G-protein and arrestin-dependent diversity of NOPR signaling provides a vital roadmap for future studies exploring the potential for functionally selective NOPR ligands as have been recently reported for numerous other GPCR systems including other opioid receptor subtypes (2, 40, 51).

In conclusion, the findings presented in this work suggest that NOPR receptors are regulated via similar but unique mechanisms as compared with the other opioid receptor subtypes. Insights gained from this study are likely to provide additional understanding of the functional properties of the nociceptin-NOPR system and signaling complex, and may be relevant to other GPCR classes and system.

Acknowledgments—We thank Gerald Zamponi (U. Calgary) for NOPR-YFP cDNA. We also thank Seva Gurevich (Vanderbilt) for technical input and all arrestin wild-type and mutant cDNA constructs. We also thank Matthew Cooper and Gina Story (Washington University) for helpful discussions, and Tiffani Palmer for help in generating stable NOPR cell lines. We also thank Children's Discovery Institute, the RNAi Consortium, and the Genome Institute at Washington University for the targeting shRNAs.

REFERENCES

1. Mollereau, C., Parmentier, M., Mailleux, P., Butour, J. L., Moisand, C., Chalon, P., Caput, D., Vassart, G., and Meunier, J. C. (1994) ORL1, a novel member of the opioid receptor family. Cloning, functional expression and localization. *FEBS Lett.* **341,** 33–38
2. Al-Hasani, R., and Bruchas, M. R. (2011) Molecular mechanisms of opioid receptor-dependent signaling and behavior. *Anesthesiology* **115,** 1363–1381
3. Reinscheid, R. K., Nothacker, H. P., Bourson, A., Ardati, A., Henningsen, R. A., Bunzow, J. R., Grandy, D. K., Langen, H., Monsma, F. J., Jr., and Civelli, O. (1995) Orphanin FQ. A neuropeptide that activates an opioid-like G protein-coupled receptor. *Science* **270,** 792–794
4. Mogil, J. S., and Pasternak, G. W. (2001) The molecular and behavioral pharmacology of the orphanin FQ/nociceptin peptide and receptor family. *Pharmacol. Rev.* **53,** 381–415
5. Altier, C., Khosravani, H., Evans, R. M., Hameed, S., Peloquin, J. B., Vartian, B. A., Chen, L., Beedle, A. M., Ferguson, S. S., Mezghrani, A., Dubel, S. J., Bourinet, E., McRory, J. E., and Zamponi, G. W. (2006) ORL1 receptor-mediated internalization of N-type calcium channels. *Nat. Neurosci.* **9,** 31–40
6. Murali, S. S., Napier, I. A., Rycroft, B. K., and Christie, M. J. (2012) Opioid-related (ORL1) receptors are enriched in a subpopulation of sensory neurons and prolonged activation produces no functional loss of surface N-type calcium channels. *J. Physiol.* **590,** 1655–1667
7. Corbani, M., Gonindard, C., and Meunier, J.-C. (2004) Ligand-regulated internalization of the opioid receptor-like 1. A confocal study. *Endocrinology* **145,** 2876–2885
8. Pierce, K. L., and Lefkowitz, R. J. (2001) Classical and new roles of β-arrestins in the regulation of G protein-coupled receptors. *Nat. Rev. Neurosci.* **2,** 727–733
9. Pierce, K. L., Premont, R. T., and Lefkowitz, R. J. (2002) Seven-transmembrane receptors. *Nat. Rev. Mol. Cell Biol.* **3,** 639–650
10. Bruchas, M. R., Macey, T. A., Lowe, J. D., and Chavkin, C. (2006) κ-Opioid receptor activation of p38 MAPK is GRK3- and arrestin-dependent in neurons and astrocytes. *J. Biol. Chem.* **281,** 18081–18089
11. Schmid, C. L., Raehal, K. M., and Bohn, L. M. (2008) Agonist-directed signaling of the serotonin 2A receptor depends on β-arrestin2 interactions *in vivo*. *Proc. Natl. Acad. Sci. U.S.A.* **105,** 1079–1084
12. Schmid, C. L., and Bohn, L. M. (2009) Physiological and pharmacological implications of β-arrestin regulation. *Pharmacol. Ther.* **121,** 285–293
13. Macey, T. A., Lowe, J. D., and Chavkin, C. (2006) μ-Opioid receptor activation of ERK1/2 is GRK3 and arrestin dependent in striatal neurons. *J. Biol. Chem.* **281,** 34515–34524
14. Rozenfeld, R., and Devi, L. A. (2007) Receptor heterodimerization leads to

a switch in signaling. β-Arrestin2-mediated ERK activation by μ-δ-opioid receptor heterodimers. *FASEB J.* **21,** 2455–2465
15. Breitman, M., Kook, S., Gimenez, L. E., Lizama, B. N., Palazzo, M. C., Gurevich, E. V., and Gurevich, V. V. (2012) Silent scaffolds. Inhibition of JNK3 activity in the cell by a dominant-negative arrestin-3 mutant. *J. Biol. Chem.* **287,** 19653–19664
16. Seo, J., Tsakem, E. L., Breitman, M., and Gurevich, V. V. (2011) Identification of arrestin-3-specific residues necessary for JNK3 kinase activation. *J. Biol. Chem.* **286,** 27894–27901
17. Zhan, X., Kaoud, T. S., Dalby, K. N., and Gurevich, V. V. (2011) Nonvisual arrestins function as simple scaffolds assembling the MKK4-JNK3α2 signaling complex. *Biochemistry* **50,** 10520–10529
18. Davies, C., and Tournier, C. (2012) Exploring the function of the JNK (c-Jun N-terminal kinase) signaling pathway in physiological and pathological processes to design novel therapeutic strategies. *Biochem. Soc. Trans.* **40,** 85–89
19. Melief, E. J., Miyatake, M., Bruchas, M. R., and Chavkin, C. (2010) Ligand-directed c-Jun N-terminal kinase activation disrupts opioid receptor signaling. *Proc. Natl. Acad. Sci. U.S.A.* **107,** 11608–11613
20. Bohn, L. M., Gainetdinov, R. R., and Caron, M. G. (2004) G protein-coupled receptor kinase/β-arrestin systems and drugs of abuse. Psychostimulant and opiate studies in knockout mice. *Neuromolecular Med.* **5,** 41–50
21. Schmid, C. L., and Bohn, L. M. (2010) Serotonin, but not *N*-methyltryptamines, activates the serotonin 2A receptor via a β-arrestin2/Src/Akt signaling complex *in vivo*. *J. Neurosci.* **30,** 13513–13524
22. Shenoy, S. K., and Lefkowitz, R. J. (2011) β-Arrestin-mediated receptor trafficking and signal transduction. *Trends Pharmacol. Sci.* **32,** 521–533
23. Celver, J., Vishnivetskiy, S. A., Chavkin, C., and Gurevich, V. V. (2002) Conservation of the phosphate-sensitive elements in the arrestin family of proteins. *J. Biol. Chem.* **277,** 9043–9048
24. Pan, L., Gurevich, E. V., and Gurevich, V. V. (2003) The nature of the arrestin X receptor complex determines the ultimate fate of the internalized receptor. *J. Biol. Chem.* **278,** 11623–11632
25. Carter, J. M., Gurevich, V. V., Prossnitz, E. R., and Engen, J. R. (2005) Conformational differences between arrestin2 and pre-activated mutants as revealed by hydrogen exchange mass spectrometry. *J. Mol. Biol.* **351,** 865–878
26. Song, X., Raman, D., Gurevich, E. V., Vishnivetskiy, S. A., and Gurevich, V. V. (2006) Visual and both non-visual arrestins in their "inactive" conformation bind JNK3 and Mdm2 and relocalize them from the nucleus to the cytoplasm. *J. Biol. Chem.* **281,** 21491–21499
27. Gurevich, V. V., Pals-Rylaarsdam, R., Benovic, J. L., Hosey, M. M., and Onorato, J. J. (1997) Agonist-receptor-arrestin, an alternative ternary complex with high agonist affinity. *J. Biol. Chem.* **272,** 28849–28852
28. Law, P. Y., Hom, D. S., and Loh, H. H. (1982) Loss of opiate receptor activity in neuroblastoma X glioma NG108-15 hybrid cells after chronic opiate treatment. A multiple-step process. *Mol. Pharmacol.* **22,** 1–4
29. McLaughlin, J. P., Xu, M., Mackie, K., and Chavkin, C. (2003) Phosphorylation of a carboxyl-terminal serine within the κ-opioid receptor produces desensitization and internalization. *J. Biol. Chem.* **278,** 34631–34640
30. Land, B. B., Bruchas, M. R., Schattauer, S., Giardino, W. J., Aita, M., Messinger, D., Hnasko, T. S., Palmiter, R. D., and Chavkin, C. (2009) Activation of the kappa opioid receptor in the dorsal raphe nucleus mediates the aversive effects of stress and reinstates drug seeking. *Proc. Natl. Acad. Sci. U.S.A.* **106,** 19168–19173
31. Grecksch, G., Just, S., Pierstorff, C., Imhof, A.-K., Glück, L., Doll, C., Lupp, A., Becker, A., Koch, T., Stumm, R., Höllt, V., and Schulz, S. (2011) Analgesic tolerance to high-efficacy agonists but not to morphine is diminished in phosphorylation-deficient S375A μ-opioid receptor knock-in mice. *J. Neurosci.* **31,** 13890–13896
32. Connor, M., Yeo, A., and Henderson, G. (1996) The effect of nociceptin on Ca^{2+} channel current and intracellular Ca^{2+} in the SH-SY5Y human neuroblastoma cell line. *Br. J. Pharmacol.* **118,** 205–207
33. Marinissen, M. J., and Gutkind, J. S. (2001) G protein-coupled receptors and signaling networks. Emerging paradigms. *Trends Pharmacol. Sci.* **22,** 368–376
34. Groer, C. E., Schmid, C. L., Jaeger, A. M., and Bohn, L. M. (2011) Agonist-directed interactions with specific β-arrestins determine μ-opioid receptor trafficking, ubiquitination, and dephosphorylation. *J. Biol. Chem.* **286,** 31731–31741
35. McLennan, G. P., Kiss, A., Miyatake, M., Belcheva, M. M., Chambers, K. T., Pozek, J. J., Mohabbat, Y., Moyer, R. A., Bohn, L. M., and Coscia, C. J. (2008) κ-Opioids promote the proliferation of astrocytes via Gβγ and β-arrestin 2-dependent MAPK-mediated pathways. *J. Neurochem.* **107,** 1753–1765
36. Bruchas, M. R., Schindler, A. G., Shankar, H., Messinger, D. I., Miyatake, M., Land, B. B., Lemos, J. C., Hagan, C. E., Neumaier, J. F., Quintana, A., Palmiter, R. D., and Chavkin, C. (2011) Selective p38α MAPK deletion in serotonergic neurons produces stress resilience in models of depression and addiction. *Neuron* **71,** 498–511
37. Goeldner, C., Reiss, D., Wichmann, J., Meziane, H., Kieffer, B. L., and Ouagazzal, A.-M. (2008) Nociceptin receptor impairs recognition memory via interaction with NMDA receptor-dependent mitogen-activated protein kinase/extracellular signal-regulated kinase signaling in the hippocampus. *J. Neurosci.* **28,** 2190–2198
38. Zhang, Z., Xin, S. M., Wu, G. X., Zhang, W. B., Ma, L., and Pei, G. (1999) Endogenous δ-opioid and ORL1 receptors couple to phosphorylation and activation of p38 MAPK in NG108-15 cells and this is regulated by protein kinase A and protein kinase C. *J. Neurochem.* **73,** 1502–1509
39. Chan, A. S., and Wong, Y. H. (2000) Regulation of c-Jun N-terminal kinase by the ORL(1) receptor through multiple G proteins. *J. Pharmacol. Exp. Ther.* **295,** 1094–1100
40. Bruchas, M. R., and Chavkin, C. (2010) Kinase cascades and ligand-directed signaling at the κ-opioid receptor. *Psychopharmacology* **210,** 137–147
41. Bruchas, M. R., Land, B. B., Aita, M., Xu, M., Barot, S. K., Li, S., and Chavkin, C. (2007) Stress-induced p38 mitogen-activated protein kinase activation mediates κ-opioid-dependent dysphoria. *J. Neurosci.* **27,** 11614–11623
42. Nobles, K. N., Xiao, K., Ahn, S., Shukla, A. K., Lam, C. M., Rajagopal, S., Strachan, R. T., Huang, T.-Y., Bressler, E. A., Hara, M. R., Shenoy, S. K., Gygi, S. P., and Lefkowitz, R. J. (2011) Distinct phosphorylation sites on the β_2-adrenergic receptor establish a barcode that encodes differential functions of β-arrestin. *Sci. Signal* **4,** ra51
43. Lau, E. K., Trester-Zedlitz, M., Trinidad, J. C., Kotowski, S. J., Krutchinsky, A. N., Burlingame, A. L., and von Zastrow, M. (2011) Quantitative encoding of the effect of a partial agonist on individual opioid receptors by multisite phosphorylation and threshold detection. *Sci. Signal.* **4,** ra52
44. Wolfe, B. L., and Trejo, J. (2007) Clathrin-dependent mechanisms of G protein-coupled receptor endocytosis. *Traffic* **8,** 462–470
45. Tibbles, L. A., and Woodgett, J. R. (1999) The stress-activated protein kinase pathways. *Cell. Mol. Life Sci.* **55,** 1230–1254
46. Manassero, G., Repetto, I. E., Cobianchi, S., Valsecchi, V., Bonny, C., Rossi, F., and Vercelli, A. (2012) Role of JNK isoforms in the development of neuropathic pain following sciatic nerve transection in the mouse. *Molecular Pain* **8,** 39
47. Antoniou, X., Falconi, M., Di Marino, D., and Borsello, T. (2011) JNK3 as a therapeutic target for neurodegenerative diseases. *J. Alzheimers Dis.* **24,** 633–642
48. Marti, M., Mela, F., Veronesi, C., Guerrini, R., Salvadori, S., Federici, M., Mercuri, N. B., Rizzi, A., Franchi, G., Beani, L., Bianchi, C., and Morari, M. (2004) Blockade of nociceptin/orphanin FQ receptor signaling in rat substantia nigra pars reticulata stimulates nigrostriatal dopaminergic transmission and motor behavior. *J. Neurosci.* **24,** 6659–6666
49. Mika, J., Obara, I., and Przewlocka, B. (2011) The role of nociceptin and dynorphin in chronic pain. Implications of neuro-glial interaction. *Neuropeptides* **45,** 247–261
50. Thompson, A. A., Liu, W., Chun, E., Katritch, V., Wu, H., Vardy, E., Huang, X.-P., Trapella, C., Guerrini, R., Calo, G., Roth, B. L., Cherezov, V., and Stevens, R. C. (2012) Structure of the nociceptin/orphanin FQ receptor in complex with a peptide mimetic. *Nature* **485,** 395–399
51. Urban, J. D., Clarke, W. P., von Zastrow, M., Nichols, D. E., Kobilka, B., Weinstein, H., Javitch, J. A., Roth, B. L., Christopoulos, A., Sexton, P. M., Miller, K. J., Spedding, M., and Mailman, R. B. (2007) Functional selectivity and classical concepts of quantitative pharmacology. *J. Pharmacol. Exp. Ther.* **320,** 1–13